

# Thermal, spectroscopic, and dissolution studies of ketoconazole–Pluronic F127 system

Bożena Karolewicz · Agata Górniak ·  
Artur Owczarek · Ewa Żurawska-Plaksej ·  
Agnieszka Piwowar · Janusz Pluta

Received: 10 July 2013 / Accepted: 15 January 2014 / Published online: 8 February 2014  
© The Author(s) 2014. This article is published with open access at Springerlink.com

**Abstract** One strategy for improving the dissolution of poorly water soluble drugs is to prepare solid dispersions such as binary mixtures with hydrophilic carriers. These mixtures are generally characterized by better solubility than those of the individual components from which they are formed. In the present study, solid dispersions of ketoconazole (KET) with Pluronic F127 (PLU) were prepared by the grinding method. Solid–liquid equilibria in the system being studied were investigated by differential scanning calorimetry. A phase diagram for the whole range of compositions was constructed. The investigation revealed that ketoconazole and Pluronic F127 form a simple eutectic system containing 4.4 % w/w of ketoconazole at the eutectic point. The results of Fourier transform infrared spectroscopy and X-ray powder diffractometry studies of obtained mixtures suggest that there is no drug-carrier interaction and both components are crystalline in the solid dispersion with the whole range of composition. The prepared mixtures show an appreciable improvement of the dissolution rate of KET in 0.5 % w/v sodium lauryl sulfate. The improvement of the dissolution rate of drug is additionally increased by effective solubilization.

**Keywords** Ketoconazole · Phase diagram · Solid dispersion · Eutectic · Pluronic F127 · DSC · FTIR · XRPD · Intrinsic dissolution

## Introduction

Ketoconazole (KET) is an antifungal agent used for the treatment of local and systemic fungal infections in the form of oral tablets and suspensions, topical creams, gels, aerosols, and shampoos [1, 2]. The antimycotic effect (fungicidal or fungistatic) of ketoconazole is realized by direct fungal cell membrane damage and the inhibition of 14- $\alpha$ -demethylase, causing loss of membrane integrity and fluidity, which is the result of insufficient ergosterol biosynthesis [3]. Due to its poor water solubility ( $0.017 \text{ mg mL}^{-1}$ ) [4] and high permeability, ketoconazole is classified in the II class of the Biopharmaceutics Classification System [5, 6]. Ketoconazole's low water solubility significantly reduces both its bioavailability [7] and therapeutic effectiveness [8]. This may cause a reduction in antifungal efficacy, side effects, pharmacokinetic variability, and may develop drug resistance [9].

There are many methods reported for the improvement of solubility and dissolution rate of poorly water soluble drugs, including reducing the particle size, use of surfactant, inclusion of complexation, and obtaining solid dispersion [10]. The preparation of solid dispersions is one of the most effective and convenient techniques used for solubility enhancement of poorly soluble drugs [11–13]. Several approaches have been employed to improve the solubility of ketoconazole [8], such as preparation of solid dispersions with polyvinylpyrrolidone 17 (PVP 17) and PVP–vinyl acetate (PVP–VA64) copolymer prepared by melt extrusion [14], solid dispersions with nicotinamide

B. Karolewicz (✉) · A. Owczarek · J. Pluta  
Department of Drug Form Technology, Wrocław Medical  
University, Borowska 211A, 50-556 Wrocław, Poland  
e-mail: bozena.karolewicz@umed.wroc.pl

A. Górniak  
Department of Inorganic Chemistry, Wrocław Medical  
University, Borowska 211A, 50-556 Wrocław, Poland

E. Żurawska-Plaksej · A. Piwowar  
Department of Pharmaceutical Biochemistry, Wrocław Medical  
University, Borowska 211A, 50-556 Wrocław, Poland

[15], and inclusion complexation of ketoconazole in  $\beta$ -cyclodextrin obtained by solvent evaporation method [5]. Solid dispersions of ketoconazole are also prepared by melt fusion and solvent evaporation method with Pluronic F127 and PVP K-30 [16]; fusion, solvent evaporation, melt solvent, and kneading method with mannitol; and PEG 4000, PEG 6000, polyvinyl pyrrolidone K-30, and  $\beta$ -cyclodextrin as carrier [17, 18].

Pluronic F127 (PLU) belongs to the group of block copolymers that have been named pluronics or poloxamers and are exploited in pharmaceutical formulation as emulsifiers, solubilizers, and wetting agents for poor water soluble drugs [19, 20]. A hydrophobic drug may be solubilized with a core of micelle or conjugated to the micelle-forming polymer which leads to an increase of dissolution their substance [21].

The aim of our investigation was to conduct thermal studies of a series of mixtures of PLU-KET to determine whether the components formed the eutectic system and whether it affects the KET dissolution. The thermal studies were carried out by differential scanning calorimetry (DSC) which is the most commonly and effectively used method for phase diagram evaluations [22]. An intrinsic dissolution (ID) study was carried out to evaluate the drug release rate from the examined dispersions. Fourier transform infrared spectroscopy (FTIR) and X-ray powder diffractometry (XRPD) of pure ketoconazole and its mixture with Pluronic F127 were used to examine whether there are chemical interactions between components in its solid state and the possibility of forming terminal solid solutions.

## Experimental

### Materials

Ketoconazole was donated by Hasco-Lek (Poland) as a gift sample. Pluronic F127 was supplied from Sigma-Aldrich (USA). Sodium lauryl sulfate (SLS) was purchased from P.P.H. "Stanlab" (Poland).

### Preparation of mixtures

Finely powdered mixtures were prepared from accurately weighed quantities of each component using a Mettler Toledo AT 261 microbalance ( $\pm 0.01$  mg). The total mass of each mixture was 5.0 g. Next, they were very thoroughly ground together for at least 10 min using an agate mortar and pestle. DSC studies confirmed that both components were stable after grounding. Ten binary mixtures of Pluronic F127 and ketoconazole were prepared. The mass ratios of the mixtures were 95.0/5.0, 90.0/10.0, 80.0/20.0, 70.0/30.0, 60.0/30.0, 50.0/50.0, 40.0/60.0, 30.0/70.0, 20.0/80.0, and

10.0/90.0 %, respectively. The mixtures were sieved through a 315  $\mu\text{m}$ -sized mesh and were stored in a desiccator over calcium chloride at room temperature until use.

### Drug content

Solid dispersions equivalent to 20 mg of ketoconazole were dissolved in 50 mL of methanol. The received solutions were determined at 245 nm by a UV-Vis spectrophotometer (Jasco V-650, Japan). The ketoconazole content of the formulations was found to be in the range of 98.9–101.8 % of the declared amount.

### Differential scanning calorimetry (DSC)

The DSC curves of each mixture were obtained using a differential scanning calorimeter (Mettler Toledo DSC 25), equipped with a heat flow sensor, and joined via the TA Controller TC 15 interface to a computer. Measurements were driven by STAR<sup>e</sup> software.

Samples for DSC measurements were weighed using a Mettler Toledo AT 261 microbalance ( $\pm 0.01$  mg) and sealed in 40  $\mu\text{L}$  standard aluminum crucibles with a single hole punched in the lid. The total mass of a sample was between 4 and 10 mg. An empty pan of the same type was employed as a reference. The DSC instrument was calibrated using the melting point of indium ( $156.6 \pm 0.3$ ) as a standard. DSC scans of each mixture were performed at a heating rate of  $5\text{ }^\circ\text{C min}^{-1}$  in the temperature range of 25–200  $^\circ\text{C}$ . The DSC cell was purged with a stream of dry argon at a rate of  $50\text{ mL min}^{-1}$ . Experiments were performed in triplicate and the mean values were calculated.

### Spectroscopic studies

#### *X-ray powder diffractometry (XRPD)*

Powder diffraction patterns were performed over the range  $2\theta$  of  $2^\circ$ – $50^\circ$ , at counting time  $1.5$ – $3\text{ min}^{-1}$ , using a Bruker D8 ADVANCE powder diffractometer, with  $\text{CuK}\alpha$  and a Vantec position sensitive detector.

#### *Fourier transform infrared spectroscopy (FTIR)*

FTIR spectra were obtained using a Shimadzu IRAffinity-1 spectrophotometer. Samples were mixed with potassium bromide and compressed into a disk using a Specac (USA) hydraulic press before scanning from 4000 to  $400\text{ cm}^{-1}$ .

### Intrinsic dissolution (ID) studies

ID studies were carried out for 90.0/10.0, 70.0/30.0, 50.0/50.0, 30.0/70.0, and 10.0/90.0 PLU/KET mixtures. The

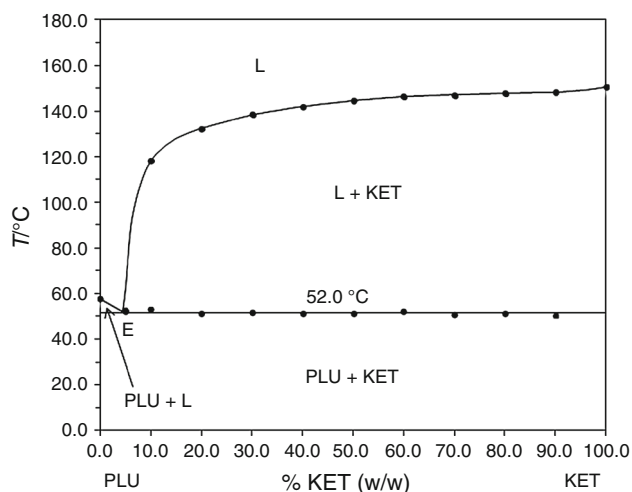
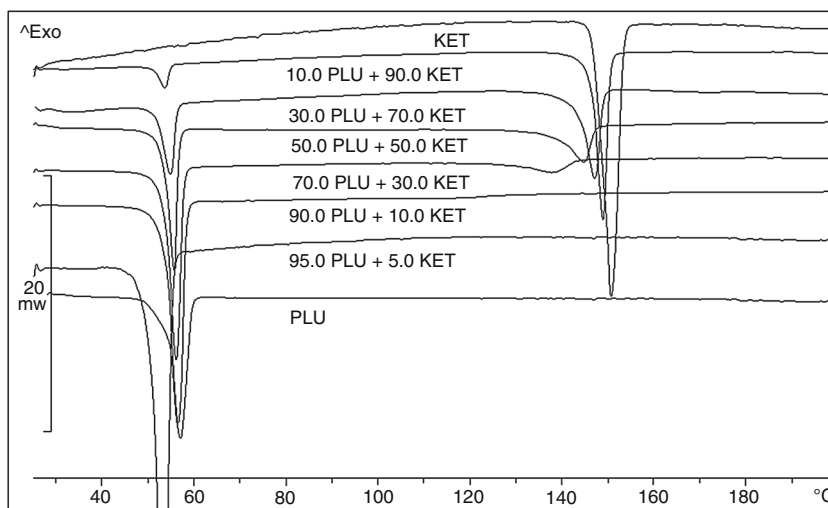


**Fig. 1** Phase equilibrium diagram of the investigated system ketoconazole (KET)–Pluronic F127 (PLU)

dissolution test was conducted under sink conditions in 1000 mL of 0.5 % SLS at  $37 \pm 0.5$  °C and a rotational speed of 50 rpm. The dissolution system was fitted with SR8-PLUS (Hanson) and 7-channel peristaltic pumps. KET (100.0 mg) or an equivalent amount of solid dispersion disks were prepared by compressing powder in a hydraulic press for 1 min under a 2 ton compression force, using a 13 mm punch. Samples were withdrawn at appropriate time intervals. The quantitative determination for KET was performed using a HPLC system with an FLD (Agilent 1100). Analysis was carried out with the use of Zorbax Eclipse XDB-C8 (Agilent). Analysis was performed by isocratic elution with a mixture of solvents on the composition of 50 mM ammonium acetate buffer (with 0.1 % formic acid and methanol) with a steady flow rate of  $1 \text{ mL min}^{-1}$ . Substances eluted from the column were identified by a fluorimetric detector at 220 nm (excitation) and 380 nm. An external standard of KET was used to

**Fig. 2** DSC curves of Pluronic F127, ketoconazole, and Pluronic F127 (PLU)—ketoconazole (KET) mixtures



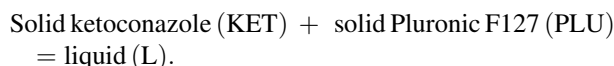
obtain a calibration curve. The evaluation method was linear in the range of  $5\text{--}80 \text{ } \mu\text{g mL}^{-1}$  (linearity  $r^2 = 0.998$ ). Dissolution experiments were performed in triplicate and the mean values were calculated.

## Results and discussion

### Thermal studies

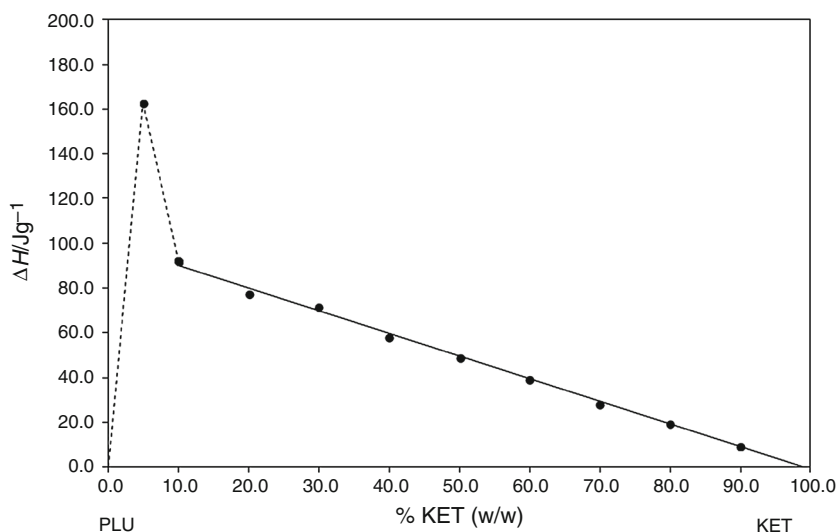
DSC curves of pure ketoconazole and Pluronic F127 obtained at a heating rate of  $5 \text{ } ^\circ\text{C min}^{-1}$  in the temperature range from 25 to 200 °C show only one sharp endothermic effect ( $\Delta_{\text{fus}}H = 45.9$  and  $86.3 \text{ kJ mol}^{-1}$ , respectively), corresponding to melting points at 150.6 and 57.4 °C, respectively. It confirms that under these conditions, the substances are stable and do not decompose.

Figure 1 shows the phase diagram of the investigated system constructed on the basis of the DSC results. Examples of DSC curves are given in Fig. 2. The DSC curves of the various mixtures clearly indicate that the investigated compounds formed a simple binary eutectic system—only two kinds of thermal effects are shown for the whole range of compositions. The onset of the first peak consistently appeared near 52.0 °C (Fig. 2), indicating a eutectic reaction:



The second peak (the temperature of liquid) was generally wider, indicating that the complete melting took place over a temperature range. Terminal solid solutions were not observed at either sides of the phase diagram. The melting points of the pure components (KET: 150.6 °C, PLU: 57.4 °C) were depressed due to the existence of the other component in the mixture as shown in the phase

**Fig. 3** Tamman's triangle construction for the eutectic melting enthalpy  $\Delta H$  at 52.0 °C



**Fig. 4** Determination of the eutectic composition in the system PLU–KET by plotting non-eutectic melting enthalpy versus mass ratio of KET

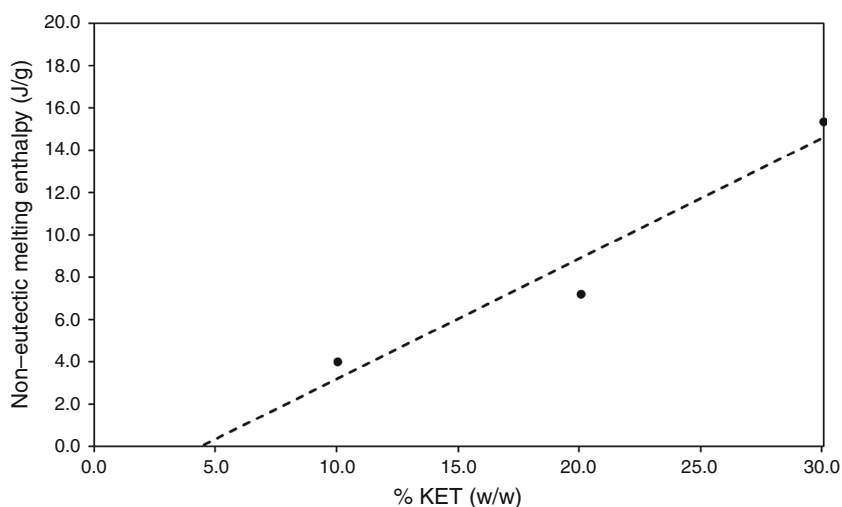
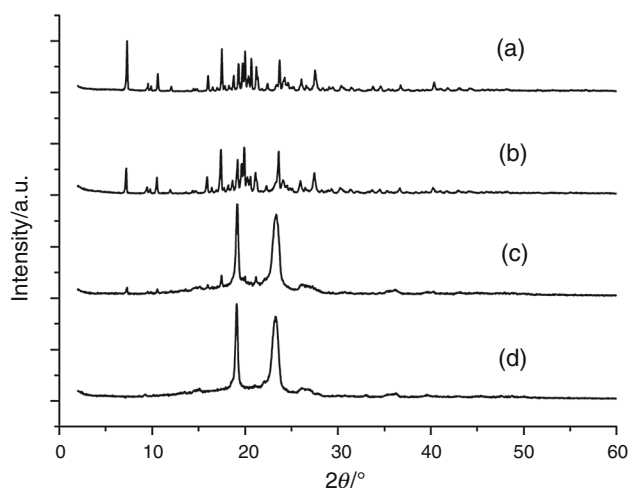
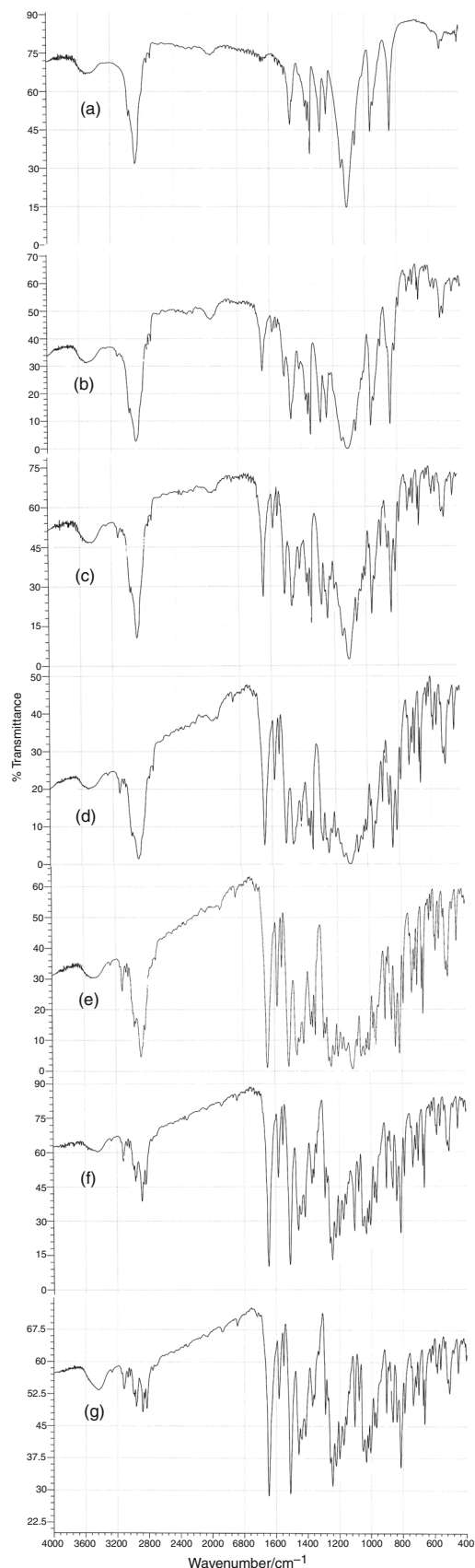


diagram in Fig. 1. The values of the eutectic melting enthalpy  $\Delta H$  for a given mixture, determined by integration of the eutectic peak area on DSC curves, are plotted in Fig. 3 versus mass fraction of KET (Tamman's triangle construction). The thermal effect of the eutectic transition goes to zero for a composition corresponding to pure KET. This confirms that there is no mutual miscibility in the solid state and no formation of a terminal solid solution. The values of the eutectic melting enthalpy  $\Delta H$  increase linearly with content of PLU and achieve a sharp rise near 5 % w/w KET. Near the eutectic point, the DSC scans showed the characteristic overlap of two endotherms (eutectic and liquidus events) into a single peak. Because of this the eutectic composition of approximately 4.4 % w/w KET was determined by plotting the non-eutectic melting enthalpy (after eutectic melting) of KET as a function of the mass percentage of the drug and extrapolating the fitted



**Fig. 5** XRPD patterns of KET (a), 10.0/90.0 % w/w PLU/KET (b), 90.0/10.0 % w/w PLU/KET (c), and PLU (d)



**Fig. 6** FTIR spectra of PLU (a), 80.0/20.0 % w/w PLU/KET (b), 60.0/40.0 % w/w PLU/KET (c), 50.0/50.0 % w/w PLU/KET (d), 30.0/70.0 % w/w PLU/KET (e), 10.0/90.0 % w/w PLU/KET (f), and KET (g)

line to zero enthalpy (Fig. 4). Finally, parameters of the eutectic point ( $E$ ) have been established as follows:

- Composition: mass fraction of KET 4.4 %, mass fraction of PLU 95.6 %;
- Temperature: 52.0 °C.

#### Spectroscopic studies

##### XRPD

The X-ray diffractograms of KET, PLU, and 10.0/90.0 % w/w PLU/KET, 90.0/10.0 % w/w PLU/KET are shown in Fig. 5. The XRPD pattern of the KET shows the crystalline nature of the drug, indicated by numerous distinctive peaks at a diffraction angle ( $2\theta$ ) at 7.30°, 10.61°, 16.04°, 17.52°, 19.31°, 19.99°, 20.66°, 21.21°, 23.77°, and 27.54°. The drug's crystalline peaks were still detectable in the mixture with PLU. The X-ray diffractogram of PLU also shows two characteristic peaks with the highest intensity at diffraction angles  $2\theta$  at 19.12° and 23.27°. The XRPD pattern for the sample containing 90.0 % w/w KET shows the presence of a slight amount of the second phase (PLU) which can be deduced from the appearance of a very weak signal at  $2\theta$  23.27° (distinctive PLU peak) and evidenced by a higher peak at  $2\theta$  19.31°. The latter effect is caused by the superposition of the line of PLU at  $2\theta$  19.12°, one of the most intensive in the PLU spectrum. On the other hand, the XRPD pattern of the sample containing 90.0 % w/w PLU shows the presence of a slight amount of crystalline KET, which can be identified by the presence of weak KET peaks at  $2\theta$  7.30°, 10.61°, 16.04°, 17.52°, 19.99°, and 21.21°. These data confirmed that at room temperature the two components which formed the investigated mixtures do not create solid solutions. Moreover, no other peaks than those which could be assigned to KET and PLU were detected on diffractograms registered for mixtures, indicating no chemical interactions in the solid state between the two entities.

##### FTIR

The FTIR spectra of the drug, carrier, and mixtures are shown in Fig. 6. The pure ketoconazole shows intense absorption bands at 1647  $\text{cm}^{-1}$  (C=O stretch), 1510  $\text{cm}^{-1}$  (C=C aromatic stretch), 1223, 1200  $\text{cm}^{-1}$  (3° amine), and 814  $\text{cm}^{-1}$  (C–Cl stretch). The FTIR spectrum of Pluronic F127 is characterized by principal absorption peaks at

**Fig. 7** Dissolution rate of KET and its mixtures with PLU

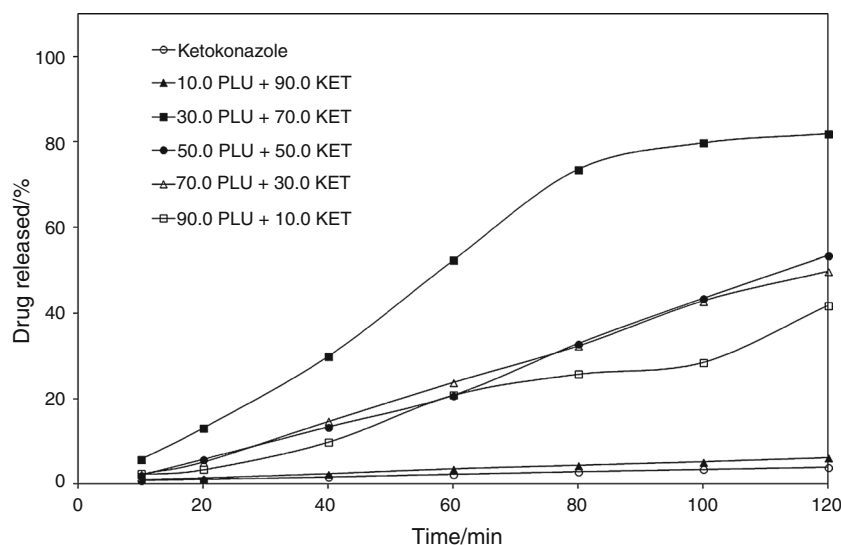


**Table 1** IDR of KET and its mixtures with PLU, and corresponding ratios

Ketoconazole/ w/w %	IDR/mg $\text{cm}^{-2} \text{min}^{-1}$	$R^2$	IDR ratio mixture/ pure drug
10.0	0.684	0.9744	12.47
30.0	0.872	0.9981	15.89
50.0	0.927	0.9930	16.88
70.0	1.495	0.9485	27.23
90.0	0.094	0.9972	1.70
100.0	0.055	0.9989	–

$R^2$  coefficient of determination

2889  $\text{cm}^{-1}$  (C–H stretching vibrations), 1342  $\text{cm}^{-1}$  (O–H bend), and 1111  $\text{cm}^{-1}$  (C–O–C stretching vibrations). All characteristic absorption bands of drug and polymer were also observed on the obtained mixtures' spectra, which show only a reduction in the sharpness of peaks as compared to the spectra of pure components. The absence of a major shift in the observed peak positions suggests the absence of interactions in the solid state between PLU and KET.

#### Intrinsic dissolution studies

The dissolution curves of KET and obtained mixtures in 0.5 % SLS at  $37 \pm 0.5$  °C are shown in Fig. 7. The intrinsic dissolution rate (IDR) of pure KET, its mixtures with PLU, and the linear relationship between the amount of the dissolved drug and time are provided in Table 1. The release rate of KET from the obtained mixtures varied with the changing ratios of drug and PLU, respectively. The rate of dissolution of pure ketoconazole was very low, less than 4 % of the drug being dissolved within 2-h dissolution

studies. The dissolution rate of the mixtures was higher compared to pure ketoconazole. For the mixture received in ratio PLU/KET 30.0/70.0, the maximum release rate of ketoconazole was the highest and IDR increases approximately 27 times in comparison with the pure drug. The mechanism of increased dissolution rates of the drug from mixtures could be related to their surface activity, wettability which may have led to reduced agglomeration, and hence increases the surface area and the solubilization effect of the carrier [23].

#### Conclusions

To our knowledge, the phase diagram for the system PLU–KET has not yet been reported. Thermal properties of some PLU–KET mixtures were already investigated by Kumar et al. [16], but the authors presented only one curve of its mixture, and the lowering of the components' melting points was not assigned to the eutectic formation.

Our DSC studies demonstrate that components of examined mixtures form a simple eutectic phase diagram. The lack of changes in FTIR and XRPD spectra indicates no chemical interaction between drug and carrier, and confirms the stability of the drug in its solid dispersions.

The dissolution results showed that the ketoconazole release was enhanced by binary mixtures adjoining to the eutectic composition which contained a higher proportion of ketoconazole than the eutectic. The impact of PLU–KET eutectic on the KET dissolution is additionally improved by effective micellization of the KET and its intimate microcrystalline eutectic mixture. The mixture containing 10 % w/w of KET is characterized by a 10-fold dissolution increase compared to the pure KET. The increase of ketoconazole release could be observed up to the mixture

containing 70 % w/w drug. Further increases of the amount of ketoconazole in the binary mixture show no significant difference on drug release compared to the drug alone. This indicates that the mixture with a mass ratio of 30/70 of PLU/KET probably has the best micellization of eutectic KET with PLU excess.

**Open Access** This article is distributed under the terms of the Creative Commons Attribution License which permits any use, distribution, and reproduction in any medium, provided the original author(s) and the source are credited.

## References

1. Heel RC, Brogden RN, Carmine A, Morley PA, Speight TM, Avery GS. Ketoconazole: a review of its therapeutic efficacy in superficial and systemic fungal infections. *Drugs*. 1982;23:1–36.
2. Odds FC, Milne LJR, Gentles JC, Ball EH. The activity in vitro and in vivo of a new imidazole antifungal, ketoconazole. *J Antimicrob Chemother*. 1980;6:97–104.
3. Kauffman A, Carver P. Use of azoles for systemic antifungal therapy. *Adv Pharmacol*. 1997;39:147–89.
4. Godefroi EF, Herees J. Inventors, Janssen Pharmaceutica, Assignee. Antifungal and antibacterial compositions of certain imidazols and methods of using same. US Patent 3,717,655. 23 July 1969.
5. Balata G, Mahdi M, Bakera RA. Improvement of solubility and dissolution properties of ketoconazole by solid dispersions and inclusion complexes. *Asian J Pharm Sci*. 2010;5:1–12.
6. Van den Mooter G, Wuyts M, Bleton N, Busson R, Grobet P, Augustijns P, Kinget R. Physical stabilisation of amorphous ketoconazole in solid dispersions with polyvinylpyrrolidone K25. *Eur J Pharm Sci*. 2001;12:261–9.
7. Chan OH, Stewart BH. Physicochemical and drug-delivery considerations for oral drug bioavailability. *Drug Discov Today*. 1996;1:461–73.
8. Yang W, Wiederhold NP, Williams RO. Drug delivery strategies for improved azole antifungal action. *Expert Opin Drug Deliv*. 2008;5:1199–216.
9. Canuto MM, Gutierrez F. Antifungal drug resistance to azoles and polyenes. *Lancet Infect Dis*. 2002;2:550–63.
10. Elder DP. Effective formulation development strategies for poorly soluble active pharmaceutical ingredients (APIs). *Am Pharm Rev*. 2010;13:28–34.
11. Alam MA, Ali R, Al-Jenoobi FI, Al-Mohizea AM. Solid dispersions: a strategy for poorly aqueous soluble drugs and technology updates. *Expert Opin Drug Deliv*. 2012;9:1419–40.
12. Górnaiak A, Wojakowska A, Karolewicz B, Pluta J. Phase diagram and dissolution studies of the fenofibrate–acetylsalicylic acid system. *J Therm Anal Calorim*. 2011;104:1195–200.
13. Górnaiak A, Karolewicz B, Żurawska-Plaksej E, Pluta J. Thermal, spectroscopic, and dissolution studies of the simvastatin–acetylsalicylic acid mixtures. *J Therm Anal Calorim*. 2013;111:2125–32.
14. Kanaujia P, Lau G, Kiong W, Widjaja E, Hanefeld A, Fischbach M, Maio M, Tan RBH. Nanoparticle formation and growth during in vitro dissolution of ketoconazole solid dispersion. *J Pharm Sci*. 2011;100:2876–85.
15. Aggarwal AK, Jain S. Physicochemical characterization and dissolution study of solid dispersions of ketoconazole with nicotinamide. *Chem Pharm Bull*. 2011;59:629–38.
16. Kumar P, Mohan Ch, Umashankar MS, Gulati M. Physicochemical characterization and release rate studies of solid dispersions of ketoconazole with Pluronic F127 and PVP K-30. *Iran J Pharm Res*. 2011;10:685–94.
17. Najmuddin M, Khan T, Mohsin AA, Shelar S, Patel V. Enhancement of dissolution rate of ketoconazole by solid dispersion technique. *Int J Pharm Pharm Sci*. 2010;3:132–6.
18. Heo M-Y, Piao Z-Z, Kim T-W, Cao Q-R, Kim A, Lee B-J. Effect of solubilizing and microemulsifying excipients in polyethylene glycol 6000 solid dispersion on enhanced dissolution and bioavailability of ketoconazole. *Arch Pharm Res*. 2005;28:604–11.
19. Adams ML, Lavasanifar A, Kwon GS. Amphiphilic block copolymers for drug delivery. *J Pharm Sci*. 2003;92:1343–55.
20. Dumortier G, Grossiord JL, Agnely F, Chaumeil JC. A review of poloxamer 407 pharmaceutical and pharmacological characteristics. *Pharm Res*. 2006;23:2709–28.
21. Saritha A, Nalini Shastri N. Preparation, physico chemical characterization of solid dispersions of tenoxicam with poloxamer. *J Pharm Sci Technol*. 2010;2:308–11.
22. Benessam S, Khimeche K, Djellouli F, Benziane M, Dahmani A. Phase diagram of ibuprofen with fatty acids. *J Therm Anal Calorim*. 2013;112:317–20.
23. Craig DQ. The mechanism of drug release from solid dispersion in water-soluble polymers. *Int J Pharm*. 2002;231:131–44.